# A Distance-Based Two-Stage Ecological Driving System Using an Estimation of Distribution Algorithm and Model Predictive Control

Hansang Lim, *Member, IEEE*, Chunting Chris Mi, *Fellow, IEEE*, and Wencong Su, *Member, IEEE*

***Abstract*—This paper proposes a distance-based two-stage ecological (eco-) driving scheme by using estimation of distribution algorithms (EDA) and model-based prediction of traffic conditions. Before departure, the optimal speed profile for an entire route is generated by an EDA in combination with speedup approaches for a faster computing time, which can optimize the complex cost function of ecodriving without simplification within a reasonably short computing time. This optimization is performed in a distance domain for localizing changes in the optimal speed profile due to traffic conditions while driving. After departure, by taking the optimal speed profile and actual traffic conditions into consideration, the speed profile for a short term—to only the next location—is adapted. In order to reliably react to actual traffic conditions, additional points are interpolated into the long-term distance step and fine control of speeds at the additional points is established, which is based on a predictive model for estimating the spacing to the preceding vehicle. The proposed ecodriving system is evaluated in two types of route conditions, and its results are compared with the optimization result by the quadratic programming method. This comparison shows that an EDA can generate a speed profile with better optimization results in terms of fuel efficiency and driving time within a shorter computing time.**

***Index Terms*—Distance based, ecodriving, estimation of distribution algorithm (EDA), long-term optimization, model predictive control (MPC), short-term adaptation.**

## I. Introduction

VEHICLES account for a large portion of total nonrenewable energy use and greenhouse gas emissions [1], and thus, fuel efficient vehicles are in high demand for energy savings and environmental concerns. Fuel consumption in a vehicle depends on various factors, such as the characteristics of its drivetrain, its operation conditions according to road and traffic conditions, and driving patterns. Therefore, drivers need to technologically be assisted in operating a vehicle in fuel efficient conditions, which is called ecodriving, and many studies on ecodriving have been reported.

Simulations have been carried out for diverse types of vehicles to analyze the optimal acceleration and cruise velocity [2]. Some studies have been conducted to change driving patterns such that they would be more ecofriendly by giving information on fuel consumption while driving. A specific guide to driving has been provided based on vehicle loading conditions [3]. Five types of feedback for ecodriving are given by using GPS and CAN bus data [4]. An onboard system which provides visual and audible warning for uneconomical driving patterns has also been developed [5].

Recent studies have focused on the optimization of a driving speed profile in order to maximize fuel efficiency. Dynamic programming (DP) is widely used as an optimization algorithm [6]–[9] since the DP method can solve the global optimization problem of a nonlinear function with complex constraints [10], [11], which corresponds to the cost function in ecodriving. Its global optimization is based on full knowledge of the entire route, including future traffic conditions, and requires long computing times. However, traffic conditions are usually changing, so future traffic conditions for the entire route are hard to anticipate exactly. This unpredictability leads to reoptimization of the speed profile in reaction to changes in traffic conditions while driving, which in turn makes global optimization using the DP method not suitable for online ecodriving.

Common approaches for online ecodriving carry out optimization over a finite horizon, i.e., a part of the route, and usually employ model predictive controls (MPCs) combined with diverse optimization algorithms. Speed profiles are optimized for varying road and traffic conditions [12] or for roads with up-down slopes [13] by using the continuation and generalized minimum residual method. The quadratic programming (QP) method is used to calculate the optimal speed profile on highways with information obtained from vehicle-to-vehicle communications [14]. Optimal speed profiles in hilly road conditions are computed by using the Legendre Pseudospectral method [15].

This optimization of a speed profile over a finite horizon shows large dependence of its optimization results on the horizon length. In order to satisfactorily improve fuel efficiency, optimization over a long horizon is preferable, major

Manuscript received July 11, 2016; revised October 18, 2016; accepted February 3, 2017. Date of publication February 10, 2017; date of current version August 11, 2017. This work was supported by the research grant of Kwangwoon University in 2016 and the Basic Science Research Program through the National Research Foundation of Korea (NRF-2016R1D1A1B03935190) and was supported in part by the U.S. Department of Energy Graduate Automotive Technology Education under Grant DE-EE0005565. The review of this paper was coordinated by D. Cao.

H. Lim is with the Department of Electronics Convergence Engineering, Kwangwoon University, Seoul 01897, South Korea (e-mail: lhs@kw.ac.kr).

C. C. Mi is with the Department of Electrical and Computer Engineering, San Diego State University, San Diego, CA 92182, USA (e-mail: cmi@sdsu.edu).

W. Su is with the Department of Electrical and Computer Engineering, University of Michigan, Dearborn, MI 48128, USA (e-mail: wencong@umich.edu).

Color versions of one or more of the figures in this paper are available online at http://ieeexplore.ieee.org.

Digital Object Identifier 10.1109/TVT.2017.2667723

challenges of which are reliable prediction of traffic conditions for the long horizon and reducing its long computing time.

For reliable prediction of future traffic conditions, traffic data obtained from communications are integrated with ecodriving on highways [14], [16]–[19]. The California Freeway Performance Measurement System [16], [17] periodically provides average traffic speed and density and the speed profile that minimizes fuel consumption and satisfies the traffic information is computed [18]. Traffic information obtained through intervehicle communication is used to predict the movement of the preceding vehicle and to compute the optimal vehicle control inputs [19]. If extended to energy managements in plug-in or hybrid electric vehicles, the trip model, i.e., the driving cycle is generated by using the archived historic traffic data on the Web which are obtained from traffic flow sensors along the freeways and the generated driving cycle is used for DP-based charge-depletion control [20], [21]. Traffic flow velocity is extracted from the average velocity of all vehicles on a specific road segment through smartphones and this real-time traffic data are utilized to calculate the optimal state-of-charge trajectory [22].

However, a long computing time cannot be avoided for a long horizon optimization, which is critical for real-time implementation. Therefore, the primary challenge in online ecodriving is to obtain satisfactory optimization results with a fast enough computing time to be implemented in real time and react to changes in traffic conditions.

An approach to overcome this challenge by optimizing the speed profile in a distance domain with a two-stage hierarchy has been made: one for long-term optimization before departure and the other for short-term adaptation while driving [23]. This work benefits from distance-based optimization to localize changes in the long-term optimal speed profile and maintain its effectiveness, except in areas under heavy traffic conditions. Short-term adaptation to follow the optimal speed and react to traffic conditions is made for the speed at only the next location, which balances the optimization and the computing time.

However, the previous work simplifies the cost function to utilize the QP method for optimization, which limits its application for diverse driving demands in terms of driving time and fuel consumption. Besides, the optimization cycle needs to be repeated in order to be in accord with changes in the vehicle status, such as gear numbers, which is estimated from initial conditions, and this repetition increases the computing time. Then, on a long trip, a step size for the short-term adaptation is so large that the vehicle may not reflect changes in the vehicle status and traffic conditions.

This paper extends this distance-based two-stage ecodriving scheme by utilizing an estimation of distribution algorithm (EDA) and MPC. A speed profile is optimized with the original, not simplified, cost function by using an EDA. Computation of the cost function is performed at each location to reflect changes in the gear numbers and not repeat the long-term optimization cycle. Then, the short-term speed is adapted with a smaller step size for more reliable driving by using a fine control framework based on interpolation and predictive model.

EDAs [24]–[27] are stochastic optimization methods which build a probability distribution from the promising populations of the previous ones and generate new populations by using the probability distribution model. This probabilistic approach speeds up the optimization process and avoids premature convergence so that EDAs can solve diverse complex problems such as the cost function in ecodriving.

The major contributions of this paper are as follows.

1) The use of an EDA is investigated for solving nonlinear, generally constrained, and computationally expensive pretrip optimization problems without simplification. To the best of our knowledge, the study of ecodriving using an EDA has not been investigated.
2) A speedup mechanism of an EDA is developed to make a faster pretrip optimization, which includes initial population generation, and selection of the optimal combination of the number of population, the iteration number, and the truncation ratio, and their simulation results are tested.
3) In order to efficiently follow the reference speed profile and reliably react to real-time traffic conditions, an MPC-based en-route fine adaptation framework is applied to the short-term adaptation. Additional locations with a small distance step are interpolated and traffic conditions in the short horizon are estimated by model-predictive control.
4) Accuracy and effectiveness of the speed profile optimization by using an EDA in the proposed ecodriving system are compared to those by using QP and the performance of the proposed ecodriving system are analyzed for diverse driving conditions.

The remainder of this paper is organized as follows. In Section II, a distance-based two-stage ecodriving scheme and its control objective are described. Section III presents the application of the EDA for long-term optimization and simulation results. In Section IV, a framework for fine control of the short-term adaptation is established, and discussions and conclusions are given in Section V.

## II. Distance-Based Two-Stage Ecodriving System

In this section, the structure of the proposed distance-based ecodriving system with two stages is presented. Then, the vehicular propulsion model and the control objective for ecodriving are derived in a distance domain.

### A. Distance-Based Ecodriving System With Two Stages

Optimization for a finite horizon of the route is a common online ecodriving approach, which deals with only a partial area of the entire route at each time for fast computing. Thus, its results are largely dependent on the horizon length [18]. A long horizon may generate more fuel efficient speed profiles rather than a short one; however, it requires a reliable prediction about traffic conditions for a long horizon, which is usually impractical and restricts its application under diverse traffic conditions. In particular, the computing time for a long horizon becomes longer, which limits the allowable horizon length for real-time implementation and, consequently, the improvement of the fuel efficiency.

Thus, an ecodriving system divided into two stages is proposed [23]. The first stage generates an optimal speed profile

for a long horizon, usually an entire route, by taking the characteristics of a drivetrain and road conditions, such as road slopes and speed limits, into consideration. If available, forecasted or historic traffic information can be used. This optimization is performed before departure so that a longer computing time is allowed in comparison with optimization while driving.

After departure, the second stage controls speeds for only a short horizon to follow the long-term optimal speed profile with consideration for actual traffic conditions, which takes a computing time short enough to be implemented in real time and makes reliable prediction of traffic conditions practical. Thus, it can produce satisfactory optimization results even though each step in the second stage calculates a short horizon.

The spacing to the preceding vehicle is used as a parameter indicating traffic conditions. In areas under smooth traffic, the speed is controlled to follow the long-term optimal speed at each location. In areas under heavy traffic, the speed is adapted to maintain the safety spacing. In order to localize effects of traffic conditions on the optimal speed profile, this ecodriving design is made in a distance domain.

In a speed profile defined in a time domain, any deviation from the optimal speed profile due to traffic conditions changes the entire reference speed after that time, which requires reoptimization for the whole remaining route. By comparison, in a speed profile defined in a distance domain, any deviation affects only areas under heavy traffic conditions and the reference speeds of other areas are still effective. That is the reason why this optimization is performed in a distance domain.

The previous two-stage-based work optimizes the speed profile by using the QP method, where the cost function is simplified into a quadratic form. This simplification limits its application to diverse driving demands. In the first-stage optimization, computations at all locations were performed all at once and the vehicle status, such as gear numbers and efficiencies of the constituent systems, are estimated from the initial speed profile. Accordingly, the optimization cycle needs to be repeated to accord with the vehicle status of the resulting speed profile, which increases the computing time. Although the first stage has a longer time budget for long-term optimization since it is performed before departure, its allowed time is still limited and the computing time is preferable to be short. In addition, the number of locations for speed control is limited such that the distance step for a long trip may be too large for proper vehicle control. Too large a distance step for control cannot reflect changes in the vehicle status, such as a gear shift, and the driving environment, such as traffic conditions.

In this study, an advanced two-stage distance-based ecodriving scheme is proposed by adding three important contributions. First, the optimization is performed with the original, not simplified, cost function by using an EDA, which can cover a wide range of driving demands. Second, the vehicle status at each location is calculated by using the actual operating conditions, such as the vehicle speed and engine speed at that location and the repetition of the optimization cycle is not required, which shortens the computing time. Third, a distance step in the long-term speed profile is divided into additional locations with a smaller step size and a fine control over them in short-term adaptation is proposed, which is based on MPC. This fine control framework can secure the safety spacing more reliably in the real-time traffic conditions.

Fig. 1 shows the overall scheme of the proposed ecodriving system. As shown in the upper panel, the entire route in the long-term optimization is composed of $(n+1)$ locations with the identical distance of $\Delta s$. The total trip distance is $n \cdot \Delta s$ and the speeds at $n$ locations are optimized for fuel consumption and driving time, the cost function of which is a nonlinear function with complex constraints. An EDA is applied to solve the optimization of this cost function without simplification within a reasonably short amount of time. Speedup approaches of an EDA are developed for faster optimization and decrease in computing time. As a result of this stage, the optimal speed profile is generated for an entire route, i.e., a sufficiently long horizon which gives a satisfactory optimized result. This generated optimal speed profile acts as a reference speed in the local adaptation.

Then, in the local adaptation, each distance step $\Delta s$ in the long-term speed profile is additionally divided into $(n_f+1)$ locations for more reliable and finer control, including the current and next locations in the long-term profile. Speeds at the $n_f$ locations in a short horizon of $\Delta s$ are controlled to follow the reference speed and keep the safety spacing to the preceding vehicle through the additional locations. The distance step in local adaptation is $\frac{\Delta s}{n_f}$, which is set to be short enough to control the vehicle reliably according to actual traffic conditions.

The vehicle performance in the local adaptation is optimized for a short horizon, but its optimization results can be satisfactorily good, since the vehicle follows the reference speed obtained from optimization for a long horizon. The reference speeds, except those for areas under heavy traffic, are still optimal and the optimality of the proposed system can be maintained even though a vehicle undergoes heavy traffic conditions in some areas.

### *B. Control Objective for Ecodriving*

Based on Willans line approximation [28], the relationships between the fuel rate and the torque, as well as the fuel rate and the engine speed, are linearly modeled and, consequently, the fuel rate $\dot{m}_f$ for an engine torque $T_e$ and an engine speed $\omega$ is modeled by [23]

$$\dot{m}_f = f(T_e, \omega) = (\beta_1 \omega + \beta_2) T_e + \gamma_1 \omega + \gamma_2 \tag{1}$$

where $\beta_1$, $\beta_2$, $\gamma_1$, and $\gamma_2$ are constants.

Since the output of this ecodriving system is a speed profile, the engine speed in (1) is replaced with a vehicle speed $v$ and (1) is modified to be

$$\dot{m}_f = \left(\beta_1 \frac{f_r g_r(n)}{r_w} v + \beta_2\right) T_e + \gamma_1 \frac{f_r g_r(n)}{r_w} v + \gamma_2 \tag{2}$$

where $f_r$ is a final drive ratio, $g_r(n)$ is a gear ratio for a given gear number $n$, and $r_w$ is a wheel radius (m).

It is assumed that a five-speed automatic transmission is installed and its gear number is set by only the current speed and the direction of the acceleration and not the amount of the

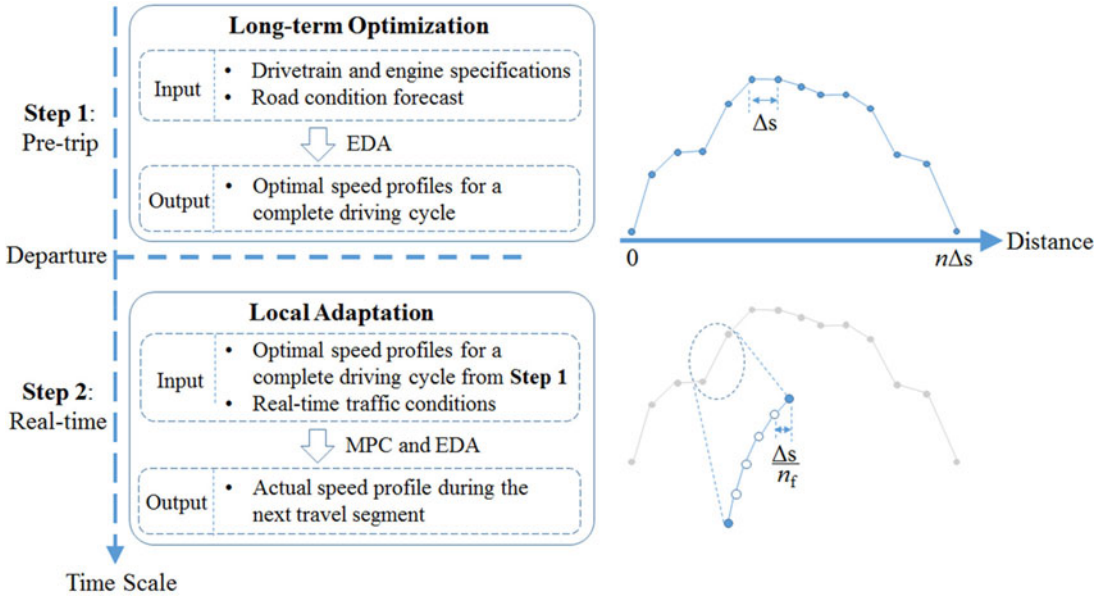


Fig. 1. Proposed two-stage distance-based ecodriving scheme.

acceleration, which means that the gear number is not the control input for optimization. To prevent the gear number from oscillating at the transition speed, the gear shift is driven with hysteresis, that is, the upshift and downshift speeds are differently set. Then, gear ratios corresponding to the first to the fifth gear numbers are 2.563, 1.552, 1.022, 0.727, and 0.52, in order.

The engine torque $T_e$ and brake force $F_{\text{brake}}$ are the inputs to control the vehicle speed $v(t)$, and their relationship can be described by

$$\begin{aligned}\dot{v}(t) = & \frac{1}{m}\left(\frac{f_r g_r(n) N_{\text{fr}} N_{\text{gr}}(n)}{r_w} T_e(t) - \frac{1}{2}\rho C_d A_d v(t)^2 \right. \\ & \left. - mgC_r \cos\theta(t) - mg\sin\theta(t) - F_{\text{brake}}(t)\right) \\ = & \frac{1}{m}\left(C_1 T_e(t) - C_2 v(t)^2 \ -C_3 - F_{\text{brake}}(t)\right) \end{aligned} \quad (3)$$

where $C_1 = \frac{f_r g_r(n) N_{\text{fr}} N_{\text{gr}}(n)}{r_w}$, $C_2 = \frac{1}{2}\rho C_d A_d$, and $C_3 = mgC_r \cos\theta(t) + mg\sin\theta(t)$. $\dot{v}(t)$is the acceleration (m/s$^2$), $N_{\text{fr}}$ is the efficiency of a final drive, and $N_{\text{gr}}(n)$ is the efficiency of the gear box and the torque converter. Then, $m$, $\rho$, $C_d$, $A_d$, $g$, $Cr$, and $\theta(t)$ are the mass of the vehicle (kg), the air density (kg/m$^3$), the drag coefficient, the frontal area of the vehicle (m$^2$), the gravity (m/s$^2$), the rolling resistance coefficient, and the road gradient (rad), in that order.

The parameters in (3) are modeled with data obtained from Autonomie, a simulation software for vehicle performance analysis developed by the Argonne National Laboratory [29]–[31]. Some parameters can be modeled as constants, which are listed in Table I.

$N_{\text{gr}}(n)$ is modeled as a product of the efficiencies of the gear box and torque converter. The efficiency of the gear box is a function of the gear number and modeled as a constant for each gear number. The efficiency of the torque converter $E_{\text{tc}}$ is modeled by the combination of a piecewise linear model and a quadratic model, as in the following:

TABLE I
PARAMETER VALUES

| Parameters | Values | Parameters | Values |
|---|---|---|---|
| $M$ | 1607 | $\rho$ | 1.19854 |
| $f_r$ | 4.438 | $C_d$ | 0.3 |
| $N_{\text{fr}}$ | 0.97 | $A_d$ | 2.25084 |
| $r_w$ | 0.30115 | $G$ | 9.81 |

$$\begin{aligned}E_{\text{tc}}(T,\omega) = & \ \min[d_1(\omega)T_i + d_2(\omega) \\ & e_1(\omega)T_i + e_2(\omega)f_1(\omega)T_i + f_2(\omega)] \end{aligned} \quad (4)$$

where $x_i(\omega) = x_{i1}\omega^2 + x_{i2}\omega + x_{i3}$ for $x = d, e, f$ and $i = 1, 2$. $T_i$ is the input torque of the torque converter and $\omega$ is the engine speed. The rolling resistance coefficient $C_r$ is modeled as a linear model of the engine speed.

Let the speed and the time at the location of $k \cdot \Delta s$ and those at the location of $(k+1)\Delta s$ be $v(k)$, $t_k$, $v(k+1)$, and $t_{k+1}$, respectively. Assume that the acceleration in a distance step between $k \cdot \Delta s$ and $(k+1)\Delta s$ is kept constant. The time difference $\Delta t_k$ between $t_{k+1}$ and $t_k$ is given by

$$\Delta t_k = t_{k+1} - t_k = \frac{2\Delta s}{v(k) + v(k+1)}. \quad (5)$$

Then, the speed at the next location is described by

$$v(k+1) = v(k) + \dot{v}(k)\frac{2\Delta s}{v(k) + v(k+1)}. \quad (6)$$

By multiplying by $v(k) + v(k+1)$ on both sides and inserting (3), the relationship between the next speed and control inputs,

such as $T_e$ and $F_{\text{brake}}$, is derived by

$$\begin{aligned} v(k+1)^2 =& \left(1-\frac{2C_2\Delta s}{m}\right)v(k)^2 \\ &+ \left[\frac{2C_1\Delta s}{m}, -\frac{2\Delta s}{m}\right]\begin{bmatrix} T_e(k) \\ F_{\text{brake}}(k)\end{bmatrix} - \frac{2C_3\Delta s}{m} \\ =& \bar{A}v(k)^2 + \bar{B}_1 T_e(k) + \bar{B}_2 F_{\text{brake}}(k) + \bar{C} \end{aligned} \tag{7}$$

where $\bar{A} = 1 - \frac{2C_2\Delta s}{m}$, $\bar{B}_1 = \frac{2C_1\Delta s}{m}$, $\bar{B}_2 = -\frac{2\Delta s}{m}$, and $\bar{C} = -\frac{2C_3\Delta s}{m}$.

In the first stage, a long-term optimization is performed by balancing fuel consumption and the speed deviation from the target speed, and its cost function is defined by

$$\begin{aligned} J_{\text{opt}} =& \; w_1 \sum_{k=0}^{n-1} \dot{m}_f(k)\Delta t_k \\ &+ w_2 \sum_{k=0}^{n-1}\left(v(k+1)^2 - V_{\text{target}}(k+1)^2\right)^2 \end{aligned} \tag{8}$$

where $\text{V}_{\text{target}}$ is the target speed at the next location, which may be a speed limit or an average speed reflecting the current traffic conditions. In this study, a speed limit is used as the target speed. In (8), the first and second terms represent the fuel consumption and the speed deviation, respectively, while $w_1$ and $w_2$ are constants representing their weights. The speed deviation is related to driving time.

In the second stage, a local adaptation is performed by also taking the spacing to the preceding vehicle into account, and its cost function at the *k*th location of the long-term speed profile is defined by

$$\begin{aligned} J_{\text{adapt}} =& \; w_1 \sum_{l=0}^{n_f-1} \dot{m}_f(l)\Delta t(l) + w_2 \sum_{l=1}^{n_f}\left(v(l)^2 - {V_{\text{target}}}^*(l)^2\right)^2 \\ &+ \sum_{l=1}^{n_f} e^{w_3(S_{\text{safe}}(l) - {S_{\text{pre}}}^*(l))} \end{aligned} \tag{9}$$

where *l* is the fine location added between *k* and $(k+1)$ locations of the long-term optimal speed profile. $S_{\text{safe}}$ and $S^*_{\text{pre}}$ are the safety spacing and actual spacing to the preceding vehicle, respectively. The superscript of $*$ represents that the parameter is estimated. The third term represents the spacing related term reflecting the traffic condition. By using an exponential function for the spacing difference [19], a spacing shorter than the safety spacing is exponentially weighted.

## III. Long-Term Optimization Using an EDA

In this section, long-term optimization by using EDA is described.

### A. Application of an EDA

By inserting (2), (5), and (7) into (8), the cost function can be given by

$$\begin{aligned} J_{\text{opt}} =& \; w_1 \sum_{k=0}^{n-1}\Bigg(\left(\beta_1\frac{f_r g_r(n_g)}{r_w}v(k) + \beta_2\right)T_e(k) \\ &+ \gamma_1\frac{f_r g_r(n_g)}{r_w}v(k) + \gamma_2) \\ &\times \frac{2\Delta s}{v(k) + \sqrt{\bar{A}v(k)^2 + \bar{B}_1 T_e(k) + \bar{B}_2 F_{\text{brake}}(k) + \bar{C}}} \\ &+ w_2 \sum_{k=0}^{n-1}\Big(\bar{A}v(k)^2 + \bar{B}_1 T_e(k) + \bar{B}_2 F_{\text{brake}}(k) \\ &+ \bar{C} - V_{\text{target}}(k+1)^2\Big)^2 \end{aligned} \tag{10}$$

subject to

$$\begin{aligned} &0 \le T_e(k) \le T_{\max} \\ &0 \le F_{\text{brake}}(k) \le F_{\text{Brake(max)}} \\ &v(k) \le \text{speed limit}(k) \\ &v(0) = v(n) = 0. \end{aligned}$$

As shown in (10), this cost function is a nonlinear complex function of the control inputs of $T_e$ and $F_{\text{brake}}$. The previous work simplifies the cost function into a quadratic form to apply the QP method [23], but this simplification is valid for only limited driving demands.

In this study, an EDA is used for optimizing the cost function without simplification. Based on stochastic approaches, an EDA can optimize a nonlinear problem with complex constraints. The probability-based generation of promising samples speeds up the optimization in an EDA and gives an explicit structure to the problem.

EDAs initially generate a predefined number of samples of control inputs for all *n* locations from 0 to (*n*-1)$\Delta s$. Thus, each sample consists of *n* pairs of control inputs ($T_e$, $F_{\text{brake}}$), which is called population. The number of populations is $n_{\text{pop}}$ and values of the cost function for all samples are computed and compared.

Then, samples with smaller values of the cost function are chosen and the number of chosen samples is given by the multiplication of the number of populations and the truncation ratio $n_{\text{pop}} \times t_r$. The probability distributions, such as the average and the standard deviation, of the chosen samples are calculated. Based on the normal distribution with the calculated average and standard deviation, new $n_{\text{pop}} \times (1 - t_r)$samples are randomly generated. This process is repeated a predefined iteration number of times.

For a trip, the speed at the initial location *v*(0) should be zero. After starting from a speed of zero, the gear number at each location is determined by the current speed and the speed at the next location is estimated by (7) in each population, which are used for computing the cost function.

During an initial iteration, EDAs usually generate the populations at random, since characteristics of a target system are unknown. Based on the randomly generated initial population set, more optimal ranges of the solution are estimated by the average and standard deviation of the population set. Although the long-term optimization is performed before departure, the

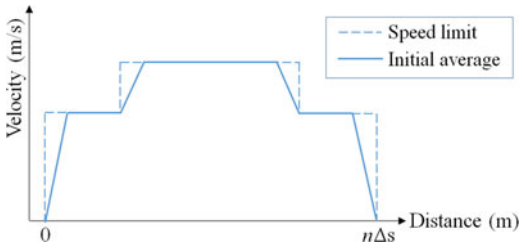


Fig. 2. Average speed estimation of the initial populations.

allowed time is still finite and it is preferable to obtain the optimization result within a shorter time.

Therefore, three approaches were adopted to shorten the computing time in applications of an EDA. First, the populations of the initial iteration are generated by the estimated possible solution area, instead of random generation. If characteristics of the target system and, consequently, the area where the possible and good solutions are located are known, the computing time for the optimal solution can be reduced. Due to the physical limit and general characteristics of the drivertrain, the possible area can be estimated and the initial populations are selected from the area.

In this study, the average values of the control inputs during the initial iteration were simply assumed by the linear acceleration and deceleration in speed transition regions, as shown in Fig. 2. The dotted and solid lines represent the speed limit and the average speed for the initial population generation.

Then, the standard deviations were assumed to be about two fifth of their maximum values, based on several simulation results. By using these estimated average and standard deviations, populations were generated and the computing time could be reduced. Smaller standard deviations increase both the possibilities that the cost function is fast optimized and the solution goes out of the optimal area. The maximum values of $T_e$ and $F_{\mathrm{brake}}$ are 220 and 3120 N $\cdot$ m, respectively, and as a result of several trials, their standard deviations were set to be 80 and 1000.

Fig. 3 shows fuel consumptions optimized by an EDA for diverse values of constituent parameters, such as the number of populations, the number of iterations $n_{\mathrm{iter}}$, and a truncation ratio. In each panel, the multiplication of the number of populations and the iteration number $n_{\mathrm{pop}}n_{\mathrm{iter}}$ is fixed, i.e., the number of samples is fixed. The circle and diamond represent the optimized results by using initial populations randomly generated and generated from the possible area which is estimated by linear acceleration and deceleration, respectively. The truncation ratio is set to be 0.5, which is a usual value.

Fuel consumption decreases as the amount of $n_{\mathrm{pop}}n_{\mathrm{iter}}$ increases. For a fixed amount of $n_{\mathrm{pop}}n_{\mathrm{iter}}$, fuel consumption decreases to some number of populations and begins to increase for larger numbers. Fuel consumption by using the estimated possible area is smaller in comparison with those of random generation. It means that the smaller number of iteration is required to obtain the same fuel consumption by using the estimated possible area and, consequently, the computing time can be shortened. The driving time and the computing time are almost same for the same $n_{\mathrm{pop}}$ and $n_{\mathrm{iter}}$ conditions.

Second, a small truncation ratio is used with sufficiently large populations. A small truncation ratio means more exchange of new samples and, accordingly, may lead to a fast conversion, but it also increases the possibility of converging to a local solution. On the other hand, as many populations are generated, samples near the global solution may be included in the populations. A small truncation ratio needs to be set by taking the relationship between the truncation ratio and the number of populations into consideration.

The relationship between them was shown in Fig. 3. The diamond and triangle represent the optimization results by using the truncation ratio of 0.5 and 0.3, respectively. Both are based on initial populations generated from the estimated possible area. For a smaller number of populations than 300, the application of the truncation ratio of 0.5 shows smaller fuel consumption but the truncation ratio of 0.3 shows better performance as the number of populations increases. For a fixed amount of $n_{\mathrm{pop}}n_{\mathrm{iter}}$, a large number of population leads to a small number of iterations, and, consequently, a short computing time. Thus, the truncation ratio was set to be 0.3 for the number of populations equal to or larger than 300.

Third, the number of populations and the iteration number were tradedoff. In EDAs, the number of calculations is the product of the number of populations and the number of iterations. The gear number and the efficiencies of the gear box and the torque converter, which are used to compute the cost function, are dependent on the current speeds and the torque inputs. For estimating those values accurately, they are calculated at each location from 0 to $n\Delta s$ in the entire route. Then, this calculation is iterated. Thus, the computing time is linearly proportional to the iteration number.

The comparison of $(n_{\mathrm{pop}}, n_{\mathrm{iter}}) = (100, 600)$ and $(200, 600)$, $(200, 300)$, and $(400, 300)$, and so on in the left panel of Fig. 4 shows that, as the number of populations increases, the computing time for each iteration increases, but it is not linearly proportional, since all populations are simultaneously calculated at each location by matrix calculation. Whereas large populations tend to shorten the iteration number required for convergence, to some extent, which decreases the computing time since the computing time is linearly proportional to the iteration number, which is shown by the comparison of $n_{\mathrm{pop}}n_{\mathrm{iter}} = 60\,000$ with $n_{\mathrm{pop}}n_{\mathrm{iter}} = 120\,000$. However, this tendency is saturated and too large populations only increase the computing time.

The relationship among the number of populations, the iteration number, and the computing time were shown in Fig. 4. As the amount of $n_{\mathrm{pop}}n_{\mathrm{iter}}$ increases, the fuel consumption decreases but the computing time increases. Considering the fuel consumption and the computing time, the number of populations and the iteration number are set to be 400 and 250, respectively.

### B. Simulations

Long-term optimization by using an EDA is implemented and solved using MATLAB. The weights $w_1$ and $w_2$ in (8) balance the effects of the fuel consumption term and speed deviation term. A relatively large value of $w_1$ gives more weight to fuel consumption and generates a speed profile with a low speed

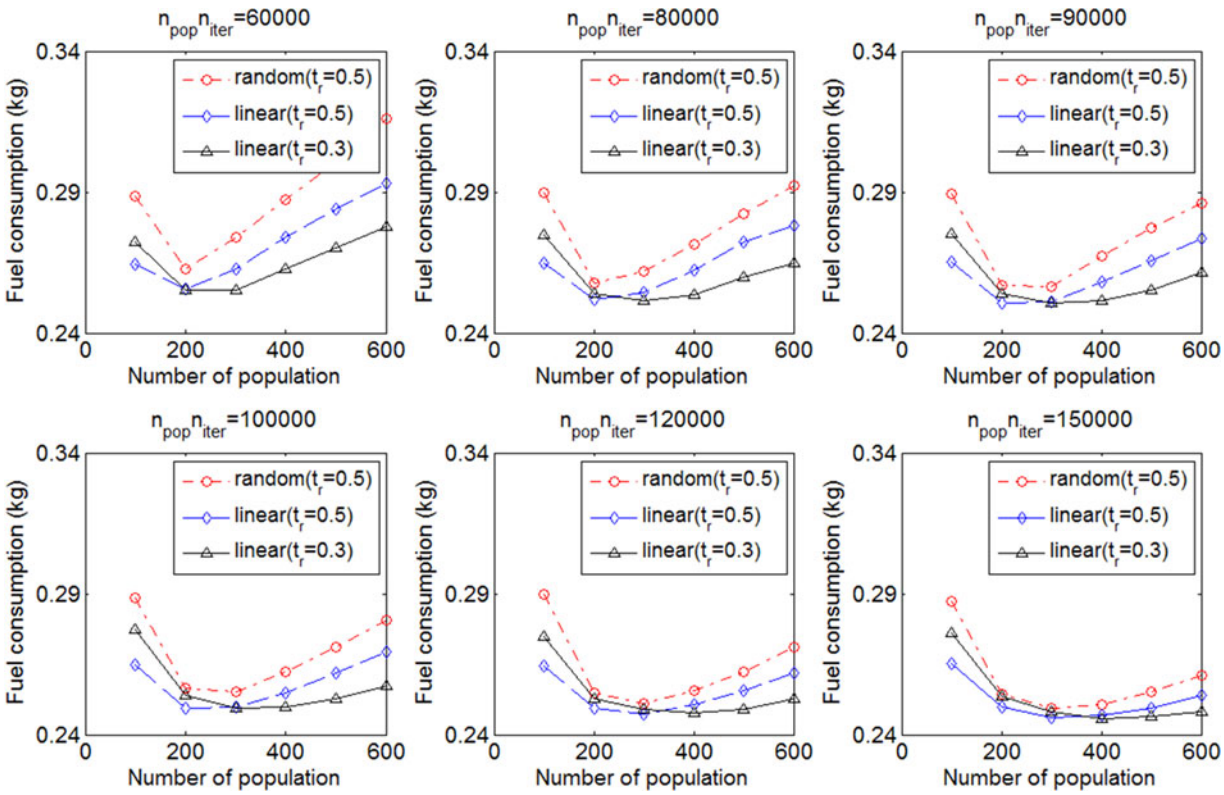


Fig. 3. Optimization results for diverse EDA parameters.

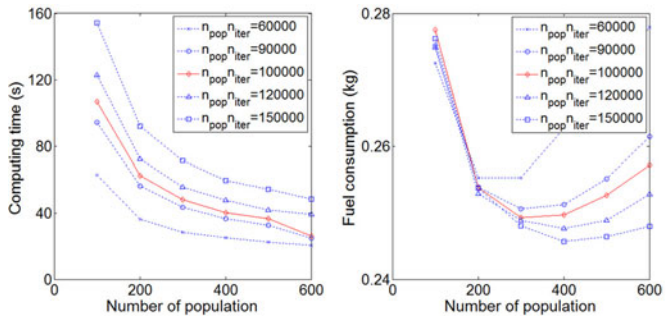


Fig. 4. Fuel consumption versus computing time.

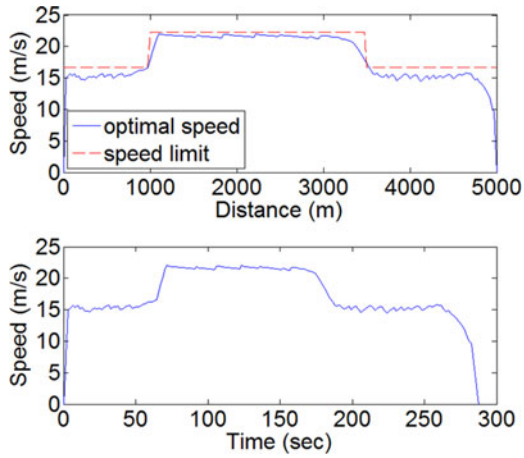


Fig. 5. Generated optimal speed profile I.

and a long driving time, which is not suitable for actual driving notwithstanding its good fuel economy since it obstructs traffic. On the other hand, a large value of $w_2$ leads to a speed profile with hard acceleration and deceleration to a target speed on each route and a short driving time, which is also not advisable due to its bad fuel economy. Therefore, a speed profile shows a tradeoff between fuel consumption and speed deviation, depending on the weight values and a good balance between them is required.

Based on simulation results for diverse values of $w_1$ and $w_2$, their values are set to be $10^8$ and 2, respectively. These values guarantees that the average speed deviations from the target speed in the steady-state regions are less than 10% and, consequently, show the best balance between fuel consumption and driving time. The final speed of the entire route should be zero. This is implemented by adding the term of $w_4(v(n+1) - 0)$ into the cost function and setting its weight $w_4$ to be $10^{10}$.

To test the validity of the proposed EDA-based ecodriving system, two driving routes were simulated. Both routes were 5 km long but had different shapes. Road gradients are assumed to be zero in the entire route. A distance step is 25 m and the total number of locations is 201.

Fig. 5 shows the optimal speed profile generated for test route I, which is a hat-shaped route. The upper and lower panels show the generated speed profile in the distance and time domain, respectively. The solid line represents the optimal speed

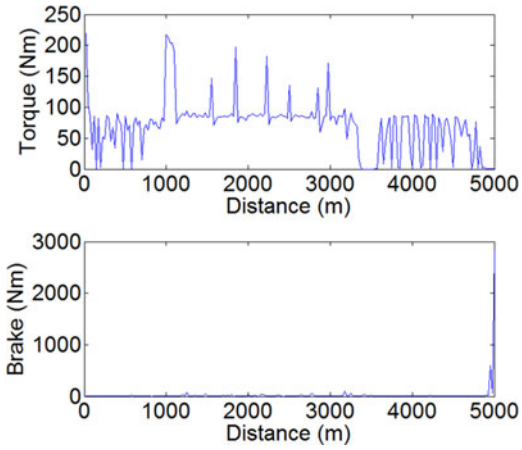


Fig. 6. Control inputs for the generated optimal speed profile.

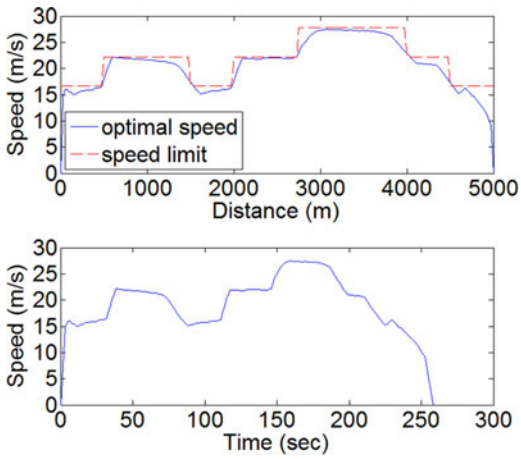


Fig. 7. Generated optimal speed profile II.

profile and the dotted line represents the speed limits, which are used as target speeds. The estimated fuel consumption was 0.250 kg and the driving time was 289 s. The computing time for this optimization was 39.9 s with an Intel i5-2467M core at a frequency of 1.6 GHz.

The engine torque and brake for this speed profile are shown in Fig. 6. The engine torque increases at the speed-up regions and goes to almost zero at the speed-down regions. At regions with a constant speed, the average engine torque is kept to be constant. It is shown that a brake force is applied only around the end region and a glide is used in the deceleration regions, which is a big advantage of optimization for a long horizon.

The optimal speed profile for test route II, which is a more complicated route, is shown in Fig. 7. The estimated fuel consumption was 0.262 kg and the driving time was 258 s. The computing time for this optimization was 40.2 s. Due to a higher speed than that of the first route, the fuel consumption increases, and the driving time decreases.

EDAs utilize random generation of populations by using a probability distribution, and the results optimized by EDAs need to be statistically analyzed. Fifty simulations were performed for each route, and Fig. 8 shows histograms of the fuel consumption, driving time, and computing time.

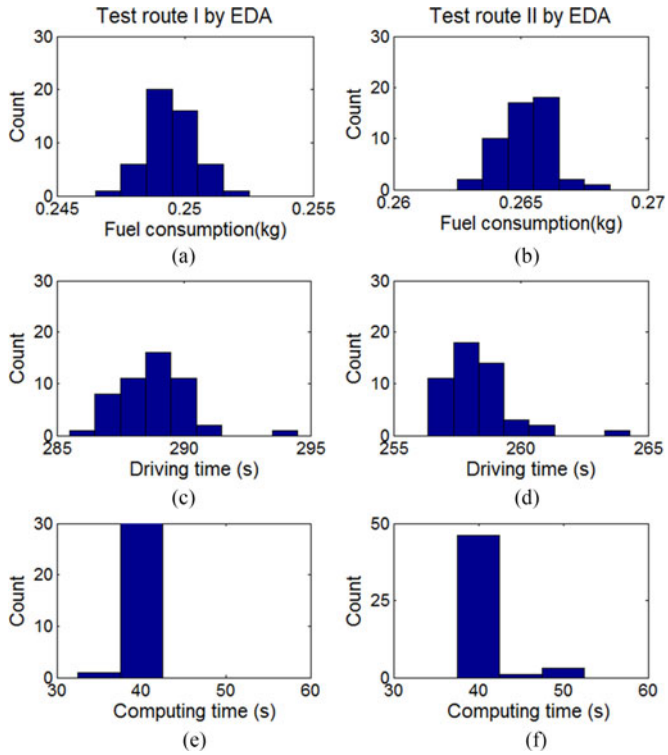


Fig. 8. Statistical analysis of optimized results by EDAs. (a) Fuel consumption (kg). (b) Fuel consumption (kg). (c) Driving time (s). (d) Driving time (s). (e) Computing time (s). (f) Computing time (s).

Fig. 8(a), (c), and (e) corresponds to the results for test route I. The average values of fuel consumption and driving time were 0.249 kg and 289 s, respectively. Their standard deviations were 0.001 and 1.32, which are less than 1% of the average values. The average computing time was 40.2 s.

Fig. 8(b), (d), and (f) corresponds to the results for test route II. The average values of fuel consumption and driving time were 0.265 kg and 258 s, respectively. Their standard deviations were 0.001 and 1.70, which were less than 1% of the average values, too. The average computing time was 41.4 s. The optimization results for both routes were statistically reliable.

### C. Comparison With QP

To validate the optimized results produced by EDAs, they are compared with the results generated by QP. The cost function in (8) is simplified into a quadratic form. Fifty QP simulations were performed for each route, and their results are shown in Fig. 9.

For test route I, the average fuel consumption and driving time in the speed profile optimized by the QP were 0.256 kg and 308 s, respectively, and their standard deviations were 0.0003 and 0.03, respectively. The computing time was 109.2 s. For test route II, the average fuel consumption and driving time were 0.265 kg and 284 s, respectively, and their standard deviations were 0.0005 and 0.0148, respectively.

As shown in (3) and (7), the gear numbers are needed for computing the cost function value. Optimization by the QP

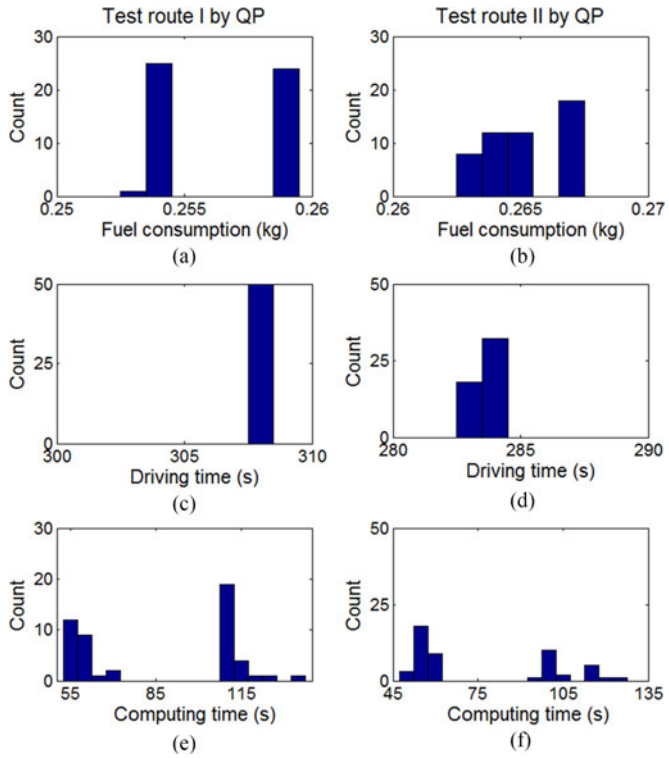


Fig. 9. Statistical analysis of optimized results by QP. (a) Fuel consumption (kg). (b) Fuel consumption (kg). (c) Driving time (s). (d) Driving time (s). (e) Computing time (s). (f) Computing time (s).

method was performed by matrix calculation and the parameter values, such as gear numbers, at all locations were required before optimization. Thus, the gear numbers were estimated from the initial condition, and optimization for the entire route was simultaneously performed by using the estimated values. The estimated parameter values were probably different from the values of the generated speed profile.

To compensate for this discrepancy in the parameter values, the optimization by QP was repeated until the parameter values were the same or the effect of the discrepancy was negligibly small. That is the reason why the computing times for QP in Fig. 9 are divided into two groups. Each optimization cycle takes less than 30 s, and the number of repeated cycles was two to five. The small computing times correspond to a group matched early to a gear number.

In comparing the EDA results with the QP results, speed profiles optimized by EDAs have better performance, but wider distribution. Average fuel consumptions are almost the same in the range from 0% to 2%, but average driving times computed by EDAs are shorter than those produced by QP by 6% to 9%. Consequently, the speed profiles generated by EDAs are better optimized.

The speed profiles generated by QP have more uniform performance though. Specifically, the driving times in all simulations are identical. Although the driving times generated by EDAs have a wider distribution, their maximum values are smaller than the driving time calculated by the QP method, and their variations are less than 1%. In particular, the fuel

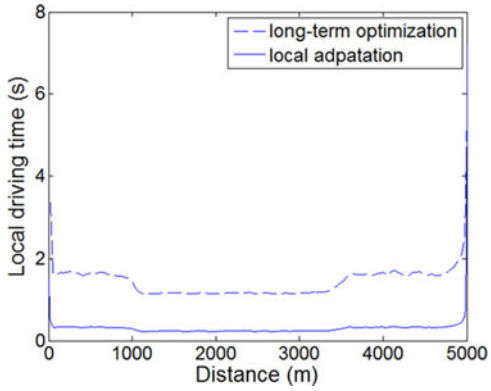


Fig. 10. Local driving times to the next location.

consumptions are almost the same, and the computing times required by EDAs are shorter than those of QP. Thus, long-term optimization by EDAs is sufficiently competitive for ecodriving.

## IV. Local Adaptation Based on MPC

While driving, the vehicle tries to follow the optimal speed profile obtained in the long-term optimization stage and locally adapts the speed according to traffic conditions for a short horizon. For more reliable and fuel efficient driving control, each distance step in the optimal speed profile is interpolated into additional locations with a smaller distance step. Fine speeds at the additional locations are generated for the short horizon.

### A. Application of MPC

Due to limit of the allowed computing time, the distance step in the optimal speed profile generated for a long route is large. A large distance step corresponds to a long local driving time from one location to the next location. The dashed line in Fig. 10 represents the local driving times in a long-term optimized speed profile. The average driving time is 1.44 s, which is too long to cope with real-time traffic conditions.

Thus, in the second stage, each distance step in the long-term optimal speed profile is divided into $n_f\ (=5)$ steps and the total number of locations where the speeds are controlled increases by $n_f$ times. The distance step in this stage is $\Delta s/n_f$ and fine controls at the additional locations are established. The solid line in Fig. 10 represents the local driving time for the fine distance step, the average value of which is 0.297 s.

The spacing to a preceding vehicle in heavy traffic conditions becomes narrower while the spacing in smooth conditions becomes wider. Thus, the spacing to the preceding vehicle is used as an index indicating traffic conditions. For safety reasons, a following vehicle maintains a minimum spacing to a preceding vehicle, which is called a safety spacing. The safety spacing is dependent on the speed of the following vehicle.

If the spacing to a preceding vehicle is farther than the safety spacing, the vehicle follows the optimal speed profile, but if the spacing is narrower than the safety spacing, the speeds are regulated to secure the safety spacing. Thus, the spacing to the

preceding vehicle is modeled by using the acceleration at the previous step.

In this study, a horizon for adaptation to traffic conditions is set to a distance step $\Delta s$ in the long-term optimal speed profile. The speed of the preceding vehicle and its spacing at each fine location are assumed to be measured. Then, the acceleration of the preceding vehicle at the $k$th location in the long-term optimal speed profile for the next $\Delta s$ horizon $a^*_{\mathrm{pre}(k)}$ is estimated to be a weighted sum of accelerations $a_{\mathrm{pre}}(l|k)$ at fine locations in the previous $\Delta s$ horizon, as in the following:

$$a^*{}_{\mathrm{pre}(k)} = \sum_{l=n_f(=-5)}^{-1} w_a(l) a_{\mathrm{pre}}(l|k), \text{ for } k = 0, \ldots, n \quad (11)$$

where $l$ represents a fine location inside the $\Delta s$ long horizon, and $w_a(l)$ is a weight. The superscript $*$ represents the estimation value.

To quickly respond to the variation in the speed of the preceding vehicle, the last two accelerations are more weighted—that is, $w_a(l) = 0.3$ for $l = -1, -2$ and $w_a(-l) = 0.2$ for $l = -3, -4, -5$. '$l < 0$', '$l = 0$', and '$l > 0$' mean the previous, current location, and next locations, respectively.

Then, the speed of the preceding vehicle $v^*_{\mathrm{pre}}(l|k)$ for the next horizon to the $(k+1)$th location is estimated by

$$v^*{}_{\mathrm{pre}}(l|k) \approx v_{\mathrm{pre}}(0|k) + a^*{}_{\mathrm{pre}(k)} \sum_{m=1}^{l} \Delta t(m|k) \quad (12)$$

for $l = 1, 2, \cdots, {}_{nf}(= 5)$, where $v_{\mathrm{pre}}(0|k)$ is the speed of the preceding vehicle at the $k$th location and $v^*_{\mathrm{pre}}(n_f|k)$ becomes the estimated speed of the preceding vehicle at the $(k+1)$th location. $\Delta t(m|k)$ is the driving time in which the following vehicle goes from the $(m-1)$th fine position to the $m$th fine position between the $k$th and $(k+1)$th locations of the long-term optimal speed profile, which is described by

$$\Delta t(m|k) = \frac{2\Delta s}{n_f\,(v(m-1|k) + v(m|k))} \quad (13)$$

where $v(\cdot)$ represents the speed of the following vehicle.

The next location of the preceding vehicle $L^*_{\mathrm{pre}}(l|k)$ can be estimated by

$$L^*{}_{\mathrm{pre}}(l|k) \approx L^*{}_{\mathrm{pre}}(l-1|k) + \frac{v_{\mathrm{pre}}(l-1|k) + v^*{}_{\mathrm{pre}}(l|k)}{2} \Delta t(l|k). \quad (14)$$

Thus, the spacing to the preceding vehicle for the next horizon $S^*_{\mathrm{pre}}(l|k)$ is estimated by

$$\begin{aligned} S^*{}_{\mathrm{pre}}(l|k) &= L^*{}_{\mathrm{pre}}(l|k) - L(l|k) \\ &= S_{\mathrm{pre}}(0|k) + \sum_{m=1}^{l} \frac{v^*{}_{\mathrm{pre}}(m-1|k) + v^*{}_{\mathrm{pre}}(m|k)}{2} \\ &\quad \times \Delta t(m|k) - l\frac{\Delta s}{n_f} \end{aligned} \quad (15)$$

and compared with the safety spacing, which is defined by [8]

$$S_{\mathrm{safe}}(l|k) = k_v \times v(l|k) + S_{\mathrm{stop}} \quad (16)$$

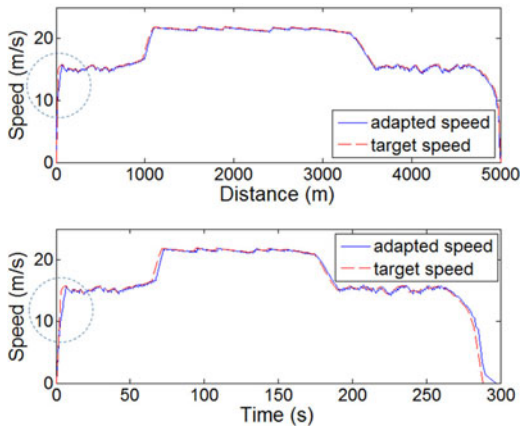


Fig. 11. Local adaptation for speed profile I under smooth traffic conditions.

where $k_v$ is a proportional constant, and $S_{\mathrm{stop}}$ is the desired spacing when the vehicle stops. Both values are set to 2.

By inserting (13)–(15) into (9), the cost function for a short horizon from the $k$th location to the $(k+1)$th location is described by

$$\begin{aligned} J_{\mathrm{adapt}}(k) = {} & w_1 \sum_{l=1}^{n_f} \dot{m}_f(l) \Delta t(l|k) \\ & + w_2 \sum_{l=1}^{n_f} \left( v(l|k)^2 - {V_{\mathrm{target}}}^*(l|k)^2 \right)^2 \\ & + \sum_{l=1}^{n_f} e^{w_3 (S_{\mathrm{safe}}(l|k) - {S_{\mathrm{pre}}}^*(l|k))}. \end{aligned} \quad (17)$$

The boundary conditions are the same as those for (10) except the initial and final speeds. The speed limit may be changed in the distance step. Thus, $\mathrm{V}_{\mathrm{target}*}(l|k)$ in (17) is given by

$${V_{\mathrm{target}}}^*(l|k) = \min(v(k), v_{\mathrm{lim}}(k)), \text{ for } k = 0, \ldots, n \quad (18)$$

where $v(k)$ is the reference speed at the $k$th location in the long-term optimal speed profile, and $v_{\mathrm{lim}}(k)$ is the speed limit at that location. The comparison between the estimated spacing and the safety spacing is implemented in the form of an exponential function in order to ensure a large effect on a closer condition than the safety spacing.

### B. Local Adaptation for Traffic Conditions

The number of populations and iterations are set as 200 and 60, respectively. The weighs are set as $w_1 = 10^5$, $w_2 = 1$, $w_3 = 10^3$, and $w_4 = 10^8$ which is the weight of the additional term $w_4(v(n_f|k) - v(k+1))$ for the final speed boundary condition. First, under smooth traffic conditions, the local adaptation was performed for optimal speed profile I with the fine distance step $\Delta \mathrm{s}/n_f$.

Fig. 11 shows that the local speeds follow the optimal long-term speed profile well, except for in the initial area indicated by a dotted circle. The estimated fuel consumption was 0.260 kg and the driving time was 297 s, which were 4% and 2% apart,

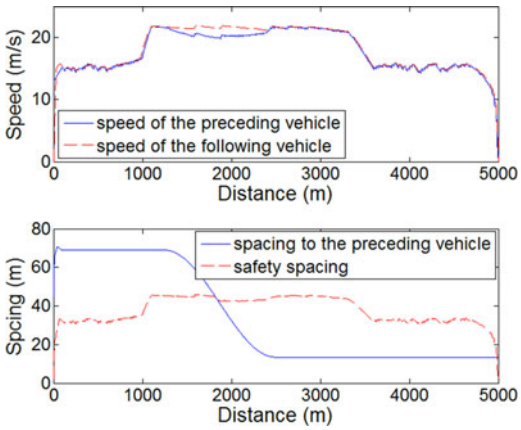


Fig. 12. Speed of the preceding vehicle and the spacing.

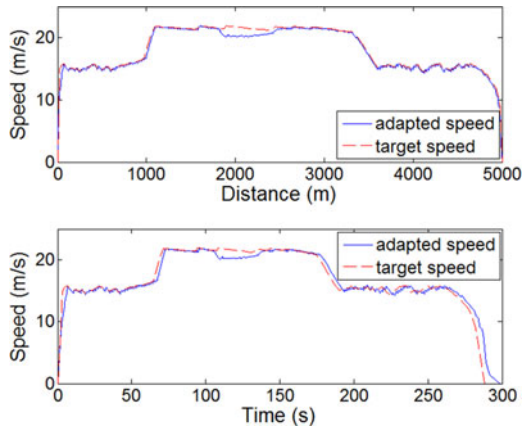


Fig. 13. Local adaptation of speed profile I under heavy traffic conditions.

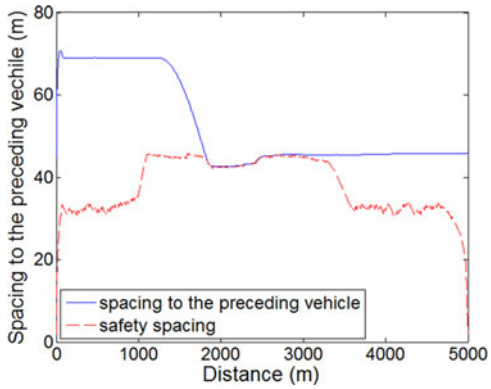


Fig. 14. Spacing to the preceding vehicle by the local adaptation.

respectively, compared to those of the long-term optimization results. This error was thought to be due to the difference in gear shift. The computing time to the next location in the long-term optimal speed profile with added $n_f$ fine locations has the average of 0.250 and the standard deviation of 0.03.

In the long-term optimization, the distance step is 25 m and a change in the speed at this distance step can be over the speed range covered by a fixed gear number. A hard acceleration area, shown in the circle of Fig. 11, actually requires the gear shift to be larger than one step. However, during each distance step, the gear is assumed to be fixed and a low gear number status allows larger torque supply for hard acceleration. Thus, the long-term optimal speed profile has a rapid increase in speed during hard acceleration, compared to that of the locally adapted speed profile, which is the reason for the small deviation.

Next, the vehicle following optimal speed profile I undergoes heavy traffic conditions in the middle of the trip. In the upper panel of Fig. 12, the solid- and dashed-lines represent the speed of the preceding vehicle and the speed of the following vehicle given by the long-term optimal speed profile, respectively. The preceding vehicle slowed down at around the 2000 m-distant areas, owing to heavy traffic. In the lower panel, the solid line represents the estimated spacing to the preceding vehicle, $S^*_{\mathrm{pre}}$, when the following vehicle keeps the long-term optimal speed without adaptation. The dashed line represents the safety spacing calculated by (16). Around the areas under heavy traffic, $S^*_{\mathrm{pre}}$ is narrower than the safety spacing such that adaptation is required.

Fig. 13 shows the locally adapted speed profile. The upper and lower panels represent the speed profile in a distance domain and a time domain, respectively. It is shown that the adapted speed is reduced around the 2000-m-distance area. The estimated fuel consumption was 0.273 kg, and the driving time was 299 s. Compared to under the smooth traffic conditions, fuel consumption increased by 5%. The computing time to the next location in the long-term optimal speed profile has the average of 0.272 and the standard deviation of 0.04.

The spacing to the preceding vehicle adapted by the locally adapted speed profile is shown in Fig. 14. Unlike the lower panel in Fig. 12, the spacing is shown to be equal to or wider than the safety spacing. The vehicle speed was controlled for securing the safety spacing around heavy traffic areas and reflected well the traffic conditions.

## V. Discussion and Conclusion

This study extends a two-stage ecological driving system optimized in a distance domain by using an EDA and MPC, which consists of a long-term optimization stage and a local adaptation stage. The former stage optimizes the speed profile for an entire trip route without consideration for traffic conditions before departure. The latter stage utilizes the optimal speed profile given by the former stage as a reference speed and adapts the reference speed for a short horizon according to actual traffic conditions while driving. In order to localize the change in the optimal speed profile due to traffic conditions, the optimization was performed in a distance domain.

The cost function for optimizing fuel consumption and driving time in a distance domain is nonlinear and complex. Therefore, an EDA was applied for optimizing the cost function without simplification, which can cover more diverse driving demands. To speed up the computing, three approaches to the application of an EDA were adopted: linearly accelerated initial conditions, a balance between the number of populations and the iteration number, and a small truncation ratio. For more

effective and reliable driving, the distance step in the long-term speed profile was interpolated and speeds at additional locations with a fine distance step were controlled in the local adaptation. The next spacing to the preceding vehicle was estimated by its weighted previous accelerations and MPC was used for optimizing the fuel consumption, the driving time, and the spacing.

This two-stage ecodriving system requires several input parameters, such as a long-term distance step and a short-term distance step. Their effects and the choice of the optimal values are the subject of future work.

## ACKNOWLEDGMENT

The authors would like to thank the anonymous reviewers for their valuable comments and suggestions to improve the quality of this paper.

## REFERENCES

[1] D. L. Greene, H. H. Baker, Jr., and S. E. Plotkin, *Reducing Greenhouse Gas Emissions From U.S. Transportation*, Center for Climate and Energy Solutions, Arlington, VA, USA, 2011.
[2] W. Y. Chou, Y. C. Lin, Y. H. Lin, and S. Y. Chen, "Intelligent eco-driving suggestion system based on vehicle loading model," in *Proc. Int. Conf. ITS Telecommun.*, Taipei, Taiwan, 2012, pp. 558–562.
[3] J. N. Hooker, "Optimal driving for single-vehicle fuel economy," *Transp. Res. Part A*, vol. 22A, no. 3, pp. 183–201, 1988.
[4] K. Jakobsen, S. C. H. Mouritsen, and K. Torp, "Evaluating eco-driving advice using GPS/CAN bus data," in *Proc. ACM SIGSPATIAL Int. Conf. Geographic Inf. Syst.*, Orlando, FL, USA, 2013, pp. 44–53.
[5] C. Vagg, C. J. Brace, D. Hari, S. Akehurst, J. Poxon, and L. Ash, "Development and field trial of a driver assistance system to encourage eco-driving in light commercial vehicle fleets," *IEEE Trans. Intell. Transp. Syst.*, vol. 14, no. 2, pp. 796–805, Jun. 2013.
[6] F. Mensing, R. Trigui, and E. Bideaux, "Vehicle trajectory optimization for application in eco-driving," in *Proc. IEEE Veh. Power Propulsion Conf.*, Chicago, IL, USA, 2011, pp. 1–6.
[7] Q. Cheng, L. Nouveliere, and O. Orfila, "A new eco-driving assistance system for a light vehicle: Energy management and speed optimization," in *Proc. IEEE Intell. Veh. Symp.*, Gold Coast, Australia, 2013, pp. 1434–1439.
[8] H. T. Luu, L. Nouveliere, and S. Mammar, "Ecological and safe driving assistance system: design and strategy," in *Proc. IEEE Intell. Veh. Symp.*, San Diego, CA, USA, 2010, pp. 129–134.
[9] F. Mensing, E. Bideaux, R. Trigui, and H. Tattegrain, "Trajectory optimization for eco-driving taking into account traffic constraints," *Transp. Res. Part D*, vol. 18, pp. 55–61, 2013.
[10] H. Zhang, J. Wang, and Y. Y. Wang, "Optimal dosing and sizing optimization for ground-vehicle diesel-engine two-cell selective catalytic reduction system," *IEEE Trans. Veh. Technol.*, vol. 65, no. 6, pp. 4740–4751, Jun. 2016.
[11] H. Zhang, P. Chen, J. Wang, and Y. Y. Wang, "Integrated study of inland-vessel diesel engine two-cell SCR systems with dynamic references," *IEEE/ASME Trans. Mechatronics*, to be published.
[12] M.A.S. Kamal, M. Mukai, J. Murata, and T. Kawabe, "On board eco-driving system for varying road-traffic environments using model predictive control," in *Proc. IEEE Int. Conf. Control Appl.*, Yokohama, Japan, 2010, pp. 1636–1641.
[13] M. A. A. Kamal, M. Mukai, J. Murata, and T. Kawabe, "Ecological vehicle control on roads with up-down slopes," *IEEE Trans. Intell. Transp. Syst.*, vol. 12, no. 3, pp. 783–794, Sep. 2011.
[14] J. Jing, "Vehicle fuel consumption optimization using model predictive control based on V2V communication," M.S. thesis, ECS Dept., The Ohio State Univ., Columbus, OH, USA, 2014.
[15] S. Xu, K. Deng, S.E. Li, S. Li, and B. Cheng, "Legendre pseudospectral computation of optimal speed profiles for vehicle eco-driving system," in *Proc. IEEE Intell. Veh. Symp.*, Dearborn, MI, USA, 2014, pp. 1103–1108.
[16] T. Choe, A. Skabardonis, and P. Varaiya, *Freeway Performance Measurement System (PeMS): An Operational Analysis Tool*, University of California, Berkeley, CA, USA, Jan. 2001.
[17] California Department of Transportation. PeMS. Oct. 2016. [Online]. Available: http://pems.dot.ca.gov
[18] N. J. Kohut, J. K. Hedrick, and F. Borrelli, "Integrating traffic data and mode predictive control to improve fuel economy," in *Proc. 12th IFAC Symp. Control Transp. Syst.*, Redondo Beach, CA, USA, 2009, pp. 155–160.
[19] M. A. S. Kamal, M. Mukai, J. Murata, and T. Kawabe, "Model predictive control of vehicles on urban roads for improved fuel economy," *IEEE Trans. Control Syst. Technol.*, vol. 21, no. 3, pp. 831–841, May 2013.
[20] Q. Gong, Y. Li, and Z. R. Peng, "Trip-based optimal power management of plug-in hybrid electric vehicles," *IEEE Trans. Veh. Technol.*, vol. 57, no. 6, pp. 3393–3401, Nov. 2008.
[21] Q. Gong, Y. Li, and Z. R. Peng, "Trip based power management of plug-in hybrid electric vehicle with two-scale dynamic programming," in *Proc. IEEE Veh. Power Propulsion Conf.*, Arlington, TX, USA, 2007, pp. 12–19.
[22] C. Sun, S. J. Moura, X. Hu, J. K. Hedrick, and F. Sun, "Dynamic traffic feedback data enabled energy management in plug-in hybrid electric vehicles," *IEEE Trans. Control Syst. Technol.*, vol. 23, no. 3, pp. 1075–1086, May 2015.
[23] H. Lim, W. Su, and C. C. Mi, "Distance-based ecological driving scheme using a two-stage hierarchy for long-term optimization and short-term adaptation," *IEEE Trans. Veh. Technol.*, to be published.
[24] T. K. Paul and H. Iba, "Linear and combinatorial optimizations by estimation of distribution algorithms," in *Proc. 9th MPS Symp. Evol. Comput.*, Japan, 2002, pp. 99–106.
[25] M. Hauschild and M. Pelikan, "An introduction and survey of estimation of distribution algorithms," *Swarm Evol. Comput.*, vol. 1, pp. 111–128, 2011.
[26] P. Yang, K. Tang, and X. Lu, "Improving estimation of distribution of algorithm on multimodal problems by detecting promising areas," *IEEE Trans. Cybern.*, vol. 45, no. 8, pp. 1438–1448, Aug. 2015.
[27] W. Dong and X. Yao, "Unified Eigen analysis on multivariate Gaussian based estimation of distribution algorithms," *Inf. Sci.*, vol. 178, pp. 3000–3023, 2008.
[28] G. Rizzoni, L. Guzzella, and B. M. Baumann, "Unified modeling of hybrid electric vehicle drivetrains," *IEEE Trans. Mechatronics*, vol. 4, no. 3, pp. 246–257, Sep. 1999.
[29] Argonne National Lab. AUTONOMIE. Oct. 2016. [Online]. Available: http://www.autonomie.net
[30] N. Kim, A. Rousseau, and E. Rask, "Autonomie model validation with test data for 2010 Toyota Prius," in *Proc. SAE*, Detroit, MI, USA, 2012, pp. 1–14.
[31] N. Kim, M. Duoba, N. Kim, and A. Rousseau, "Validating volt PHEV model with dynamometer test data using Autonomie," *SAE Int. J. Passenger Cars*, vol. 6, no. 2, pp. 985–992, 2013.

**Hansang Lim** (M'09) received the B.S., M.S., and Ph.D. degrees from the School of Electrical Engineering, Seoul National University, Seoul, South Korea, in 1996, 1998, and 2004, respectively.

He was with the Telecommunication R&D Center, Samsung Electronics Co., Ltd., from 2004 to 2007. He is currently a Professor with the Department of Electronics Convergence Engineering, Kwangwoon University, Seoul. His research interests include instrumentation and measurement systems, vehicular electronics, and power management in electrified vehicles.

**Chunting Chris Mi** (S'00–A'01–M'01–SM'03–F'12) received the B.S.E.E. and M.S.E.E. degrees in electrical engineering from Northwestern Polytechnical University, Xi'an, China, in 1985 and 1988, respectively, and the Ph.D. degree in electrical engineering from the University of Toronto, Toronto, ON, Canada, in 2001.

He was with General Electric Company, Peterborough, ON, and a Professor with the Department of Electrical and Computer Engineering, University of Michigan, Dearborn, MI, USA. He is currently a Professor of electrical and computer engineering and the Director of the Department of Energy-funded Graduate Automotive Technology Education Center for Electric Drive Transportation, San Diego State University, San Diego, CA, USA. He has conducted extensive research and has published more than 100 journal papers. His research interests include electric drives, power electronics, electric machines, renewable-energy systems, and electrical and hybrid vehicles.

Dr. Mi is an Area Editor of the IEEE TRANSACTIONS ON VEHICULAR TECHNOLOGY and an Associate Editor of the IEEE TRANSACTIONS ON POWER ELECTRONICS and the IEEE TRANSACTIONS ON INDUSTRY APPLICATIONS.

**Wencong Su** (S'06–M'13) received the B.S. degree (with distinction) in electrical engineering from Clarkson University, Potsdam, NY, USA, in 2008; the M.S. degree in electrical engineering from Virginia Tech, Blacksburg, VA, USA, in 2009; and the Ph.D. degree in electrical engineering from North Carolina State University, Raleigh, NC, USA, in 2013.

He is currently an Assistant Professor with the Department of Electrical and Computer Engineering, University of Michigan, Dearborn, MI, USA. His research interests include power and energy systems, electrified transportation systems, cyber-physical systems, and electricity markets.